The Astrophysical Journal, 586:195–200, 2003 March 20

SELECTION OF METAL-POOR GIANT STARS USING THE SLOAN DIGITAL SKY SURVEY PHOTOMETRIC SYSTEM

Amina Helmi,[1] Željko Ivezić,[2,3] Francisco Prada,[4,5] Laura Pentericci,[4] Constance M. Rockosi,[6] Donald P. Schneider,[7] Eva K. Grebel,[4] Daniel Harbeck,[4] Robert H. Lupton,[2] James E. Gunn,[2] Gillian R. Knapp,[2] Michael A. Strauss,[2] and Jonathan Brinkmann[8]

Received 2002 September 20; accepted 2002 November 22

ABSTRACT

We present a method for the photometric selection of metal-poor halo giants from the imaging data of the Sloan Digital Sky Survey[9] (SDSS). These stars are offset from the stellar locus in the $g-r$ versus $u-g$ color-color diagram. Based on a sample of 29 candidates for which spectra were taken, we derive a selection efficiency of the order of 50% for stars brighter than $r \sim 17$ mag. The candidates selected in 400 deg^2 of sky from the SDSS Early Data Release trace the known halo structures (tidal streams from the Sagittarius dwarf galaxy and the Draco dwarf spheroidal galaxy), indicating that such a color-selected sample can be used to study the halo structure even without spectroscopic information. This method, and supplemental techniques for selecting halo stars, such as RR Lyrae stars and other blue horizontal-branch stars, can produce an unprecedented three-dimensional map of the Galactic halo based on the SDSS imaging survey.

Subject headings: Galaxy: general — Galaxy: halo — Galaxy: structure — stars: Population II — surveys — techniques: photometric

1. INTRODUCTION

Studies of the Galactic halo can help constrain the formation history of the Milky Way. Currently popular hierarchical models of galaxy formation predict the presence of substructures (tidal tails, streams) due to the mergers and accretion the Galaxy may have experienced over its lifetime (Helmi et al. 2003; Steinmetz & Navarro 2002). These structures should be ubiquitous in the outer halo, where the dynamical timescales are sufficiently long for them to remain spatially coherent (Johnston, Hernquist, & Bolte 1996; Mayer et al. 2002). The best tracers of the outer halo are the luminous giant stars (which can be detected at distances of over 100 kpc), and several investigations are taking advantage of tailored techniques, like Washington photometry (Geisler 1984), to identify these stars (e.g., Majewski et al. 2000; the Spaghetti Photometric Survey [SPS], see Morrison et al. 2000). In previous works blue horizontal-branch and RR Lyrae stars have also been used to probe the outer halo (Sommer-Larsen, Flynn, & Christensen 1994; Kinman, Suntzeff, & Kraft 1994) and even discover substructures, many of which are debris from the Sagittarius dwarf galaxy (Ivezić et al. 2000; Yanny et al. 2000; Vivas et al. 2001).

The Sloan Digital Sky Survey (SDSS; York et al. 2000) has the potential to revolutionize studies of the Galactic halo because it will provide homogeneous and deep ($r < 22.5$) photometry in five passbands (u, g, r, i, and z; Fukugita et al. 1996; Gunn et al. 1998; Smith et al. 2002; Hogg et al. 2002), accurate to a few percent of up to 10,000 deg^2 in the northern Galactic cap. The survey sky coverage will result in photometric measurements of about 50 million stars and a similar number of galaxies. Astrometric positions are accurate to better than $0\farcs1$ per coordinate (rms) for sources brighter than 20.5 mag (Pier et al. 2003). Such a large database is well suited for studies of Galactic structure, with the caveat that the photometric system must be able to identify different classes of stars and variations in their metallicity and luminosity. This separation is particularly challenging for Galactic halo tracers because the number of halo stars at a given magnitude is much smaller than that of any other Galactic component [e.g., in a high-latitude field at $b = 45°$, at $V \sim 17$ mag, and $0.3 \leq (B-V) \leq 1.5$, the fraction of halo giants is $\sim$6%; see Robin, Reylé, & Crézé 2000].

In this paper, we present a method designed to select candidate metal-poor giants based on their SDSS colors. Using a sample of known metal-poor halo giants discovered by the SPS, we isolated a region in the SDSS $g-r$ versus $u-g$ color-color diagram in which the probability of a star being a giant is enhanced. Spectroscopic observations of an unbiased sample of 29 "candidate" stars with $r < 17$ indicate that the selection efficiency of our technique is approximately 50%. In § 2 we describe the selection method, and in § 3 we discuss its implications for the Galactic halo studies.

[1] Max-Planck-Institut für Astrophysik, Karl-Schwarzchild-Strasse 1, Postfach 1317, 85741 Garching bei München, Germany. Current address: Sterrekundig Institut, Universiteit Utrecht, P.O. Box 80000, 3508 TA Utrecht, Netherlands; ahelmi@phys.uu.nl.

[2] Princeton University Observatory, Peyton Hall, Ivy Lane, Princeton, NJ 08544; ivezic@astro.princeton.edu, rhl@astro.princeton.edu, jeg@astro.princeton.edu, gk@astro.princeton.edu, strauss@astro.princeton.edu.

[3] Russell Fellow.

[4] Max-Planck-Institut für Astronomie, Königstuhl 17, 69117 Heidelberg, Germany; laura@mpia-hd.mpg.de, grebel@mpia-hd.mpg.de, harbeck@mpia-hd.mpg.de.

[5] Centro Astronómico Hispano-Alemán, Apartado 511, E-04080 Almeria, Spain; prada@caha.es.

[6] University of Washington, Deptartment of Astronomy, Box 351580, Seattle, WA 98195; cmr@astro.washington.edu.

[7] Department of Astronomy and Astrophysics, 525 Davey Laboratory, Pennsylvania State University, University Park, PA 16802; dps@astro.psu.edu.

[8] Apache Point Observatory, P.O. Box 59, Sunspot, NM 88349; jb@apo.nmsu.edu.

[9] The SDSS Web site is at http://www.sdss.org.

2. COLOR SELECTION OF METAL-POOR GIANT STARS

2.1. *The SDSS Photometric Data*

We use SDSS imaging data that were taken during the commissioning phase and which are part of the SDSS Early Data Release (Stoughton et al. 2002, hereafter EDR). We analyze here equatorial observing runs 94, 125, 752, and 756, which cover 394 deg^2 and include two regions: $|\delta_{J2000.0}| \lesssim 1\overset{\circ}{.}27$ and $\alpha_{J2000.0} = 23^h24^m$–$03^h44^m$ (runs 94 and 125) and $\alpha_{J2000.0} = 08^h7^m$–$16^h40^m$ (runs 752 and 756). In order to test the photometric repeatability, we also use run 1755, which overlaps with run 125 in the range $\alpha_{J2000.0} = 23^h22^m$–$03^h03^m$ (74.8 deg^2 area). Note that the wide range of Galactic coordinates implies that the different Galactic components will manifest themselves with varying strength within this data set.

We have extracted 2,143,248 objects classified as point sources by the photometric pipeline (*photo*; Lupton et al. 2001), which do not have any of the following flags set: *bright*, *satur*, *blended*, *notchecked*, *deblended_as_moving*. This flag combination selects sources with the most reliable photometry (for details see EDR and Ž. Ivezić et al. 2003, in preparation, hereafter Paper II). We use the "point-spread function" magnitudes corrected for interstellar reddening[10] (Schlegel, Finkbeiner, & Davis 1998).

2.2. *SDSS Colors of the SPS Giants*

Some regions observed by the SPS overlap with runs 752 and 756. The SPS's Washington photometry is used to isolate metal-poor stars on the basis of their $(M-T_2)$ and $(M-51)$ colors (sensitive to temperature and the strength of the Mg *b* and MgH features near 5200 Å, respectively; see Geisler, Claria, & Minniti 1991; Paltoglou & Bell 1994) and to obtain a first estimate of the luminosity class of the stars. These candidates are observed spectroscopically and are classified into dwarfs and giants using the following indicators (Morrison et al. 2002):

1. The Mg *b* and MgH features near 5200 Å, which are characteristic of dwarfs and are almost absent in giant stars for $0.8 \leq (B-V) \leq 1.3$ (Flynn & Morrison 1990).
2. The Ca I λ4227 line, which is usually present in dwarfs and absent in giants; while this feature may be visible in metal-poor giants (with [Fe/H] ≥ -1.5), it is much weaker than in dwarfs of the same color.
3. The Ca II H and K lines near 3950 Å, which are sensitive to [Fe/H] (see Beers et al. 1999).

The contours in the top left panel of Figure 1 show, in the $g-r$ versus $u-g$ color-color diagram, the distribution of 19,000 stars from run 125 that are brighter than $r = 19$ and whose photometric errors in all bands (u, g, and r) are less than 0.05. Nine SPS giants[11] (Dohm-Palmer et al. 2001) are shown by filled circles and are clearly offset from the center of the stellar locus (for a discussion of the position of the stellar locus in the SDSS photometric system see, e.g., Finlator et al. 2000). In the other SDSS color-color projections, the SPS giants fall right on the stellar locus, having $0.15 \leq r-i \leq 0.4$ and $0 \leq i-z \leq 0.25$. Note also that since metal-poor stars are bluer than metal-rich stars of the same temperature (see Mihalas & Binney 1981, p. 120), they are shifted left from the main locus in the $g-r$ versus $u-g$ diagram shown in Figure 1 (Lenz et al. 1998; Fan 1999).

2.3. *Definition of the s Color*

We use the well-defined stellar locus to derive a principal axes coordinate system (P_1, P_2), where P_1 lies parallel to the stellar locus and P_2 measures the distance from it (see also Odenkirchen et al. 2001; Willman et al. 2001). The origin is chosen to coincide with the highest stellar density $(u-g = 1.21, g-r = 0.42)$. Since the objects of interest occur in a relatively narrow color range, we restrict ourselves to $1.1 \leq u-g \leq 2$ and $0.3 \leq g-r \leq 0.8$ (we refer the reader to Lenz et al. 1998 for an extensive study of how the SDSS colors of stars translate into temperature, metallicity, and surface gravity). This procedure yields

$$P_1 = 0.910\ (u-g) + 0.415\ (g-r) - 1.28\ , \qquad (1)$$

$$P_2 = -0.415\ (u-g) + 0.910\ (g-r) + 0.12\ . \qquad (2)$$

The top right panel in Figure 1 shows the r versus P_2 color-magnitude diagram for 47,771 stars from run 125. The position of the locus clearly depends on the r magnitude (the median P_2 color becomes redder at the faint end), and we correct for this effect using a linear P_2 versus r fit (the correction varies from -0.03 to 0.05 mag). We thus define a new color, s—named after the Spaghetti survey—that is normalized such that its error is approximately equal to the mean photometric error in a single band (assuming uncorrelated measurements in the u, g, and r bands). We obtain

$$s = -0.249u + 0.794g - 0.555r + 0.24\ . \qquad (3)$$

The r versus s color-magnitude diagram for stars with $-0.1 < P_1 < 0.6$ is shown in the bottom left panel of Figure 1. The thick solid line in the bottom right panel of Figure 1 shows the distribution of s for stars brighter than $r = 19$ that were observed in both runs 125 and 1755. The equivalent Gaussian distribution width determined from the interquartile range is 0.035 mag. The dashed line shows the distribution of the difference in s between the two epochs divided by $\sqrt{2}$; its width is 0.025 mag; that is, the error distribution is narrower than the observed s color distribution, demonstrating that the s color distribution reflects some intrinsic stellar property. The thin solid line is a best Gaussian fit to the s color distribution and shows that the latter is not symmetric: the red wing contains more stars than the blue wing.

2.4. *The Selection Criteria for Metal-poor Giants*

Based on the s color distribution of the SPS giants and the overall s color distribution, we select candidate metal-poor giants as stars with $r < 19$, $-0.1 < P_1 < 0.6$ (for $1.1 \leq u-g \leq 2$ and $0.3 \leq g-r \leq 0.8$), and

$$s > m_s + 0.05\ , \qquad (4)$$

where m_s is the median value of s in appropriately chosen subsamples. Since the accuracy of EDR data calibration is finite (about 0.01–0.02 mag), m_s is not exactly zero. We calibrate the data corresponding to a given run and camera column (i.e., individual scan line) independently and compute m_s for these subsamples. As expected, the m_s distribution is

[10] The full reddening correction is applied because the majority of stars relevant to this study (i.e., blue stars) are expected to be farther than 1 kpc, see Finlator et al. (2000).

[11] Kindly provided to us by H. Morrison.

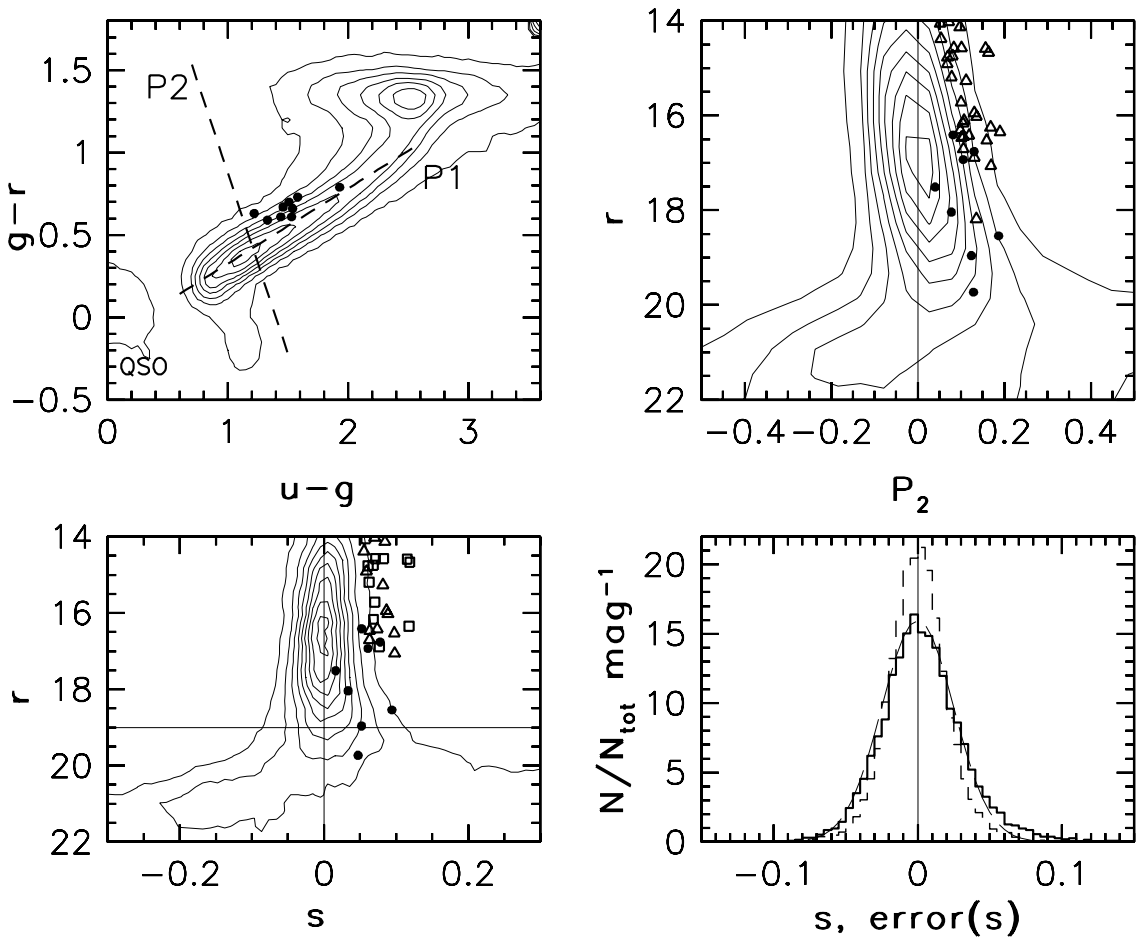

FIG. 1.—*Top left panel*: Contours show the distribution of 19,000 stars with $r < 19$ in the $g-r$ vs. $u-g$ color-color diagram. A sample of metal-poor giants discovered by the SPS is shown by solid circles (*all panels*); note that they are offset from the locus center. The dashed lines show a principal axes system aligned with the locus. *Top right panel*: r vs. P_2 color-magnitude diagram. *Bottom left panel*: s vs. P_2 diagram, where s is derived from P_2 by accounting for the magnitude dependence. The thick solid histogram in the bottom right panel shows the distribution of s for stars brighter than $r = 19$ from run 125 that were also observed in run 1755. The dashed histogram shows the s error distribution determined from multiple observations. The thin solid curve is a best Gaussian fit to the s color distribution and shows that the latter is not symmetric: the red wing has more stars than the blue wing. The candidate giants from the spectroscopic sample discussed in § 3.2 are shown by triangles in the upper right panel and divided into confirmed giants (*squares*) and dwarfs (*triangles*) in the bottom left panel.

well described by a Gaussian with a width of ~0.025 mag (see Fig. 2, *top right panel*). Note as well that m_s (or equivalently the location of the principal axes) may change slightly as a function of Galactic coordinates as a result of a different mixture of stellar populations. However, this shift is sufficiently small that we may neglect it. Hereafter, we will simply use $\hat{s}$ when referring to this median-corrected color.

3. TESTS OF THE SELECTION METHOD

3.1. *Comparisons of the Candidates and a Control Sample*

We define two samples for comparing the angular and magnitude distribution: the "candidates" $\mathscr{R}$ with $\hat{s} > +0.05$ and the "control sample" $\mathscr{B}$ with $\hat{s} < -0.05$. In all the runs that we have analyzed, we find that the number of stars in $\mathscr{R}$ is significantly larger than in $\mathscr{B}$. We compare the angular and magnitude distribution of the two samples in Figure 2 for stars in runs 752 and 756 whose photometric errors[12] in all bands (u, g, and r) are less than 0.05. To account for a smaller number of stars in $\mathscr{B}$, we have selected a random subset of $\mathscr{R}$ having the same size as $\mathscr{B}$.

The top left panels in Figure 2 show that the angular distribution of stars in $\mathscr{R}$ appears more isotropic than that of $\mathscr{B}$. In particular, the number of stars in $\mathscr{B}$ increases toward lower Galactic latitudes, indicating that they are dominated by the disk population. It is evident from the bottom left panels in the same figure that the samples have different magnitude distributions—the $\mathscr{R}$ sample contains a larger fraction of bright stars—which possibly reflects different distance distributions. These results hint at an overall different spatial distribution for stars in the candidate region from those in the control sample. The bottom right panel shows that there is an enhancement in the stellar density of the $\mathscr{R}$ sample (*dotted curve*) for $\alpha_{J2000.0}$ in the range of 13^h–16^h, which can be linked to the recently discovered clumps in the Galactic halo, associated with the Sagittarius dwarf northern tidal streams (Ivezić et al. 2000; Yanny et al. 2000; Dohm-Palmer et al. 2001; Martinez-Delgado et al. 2001; Newberg et al. 2002). We performed a χ^2 statistical test to determine the probability that the $\mathscr{B}$ and $\mathscr{R}$ samples are drawn from the same parent population. If we restrict the

[12] Here we use a newer processing rerun than available in EDR.

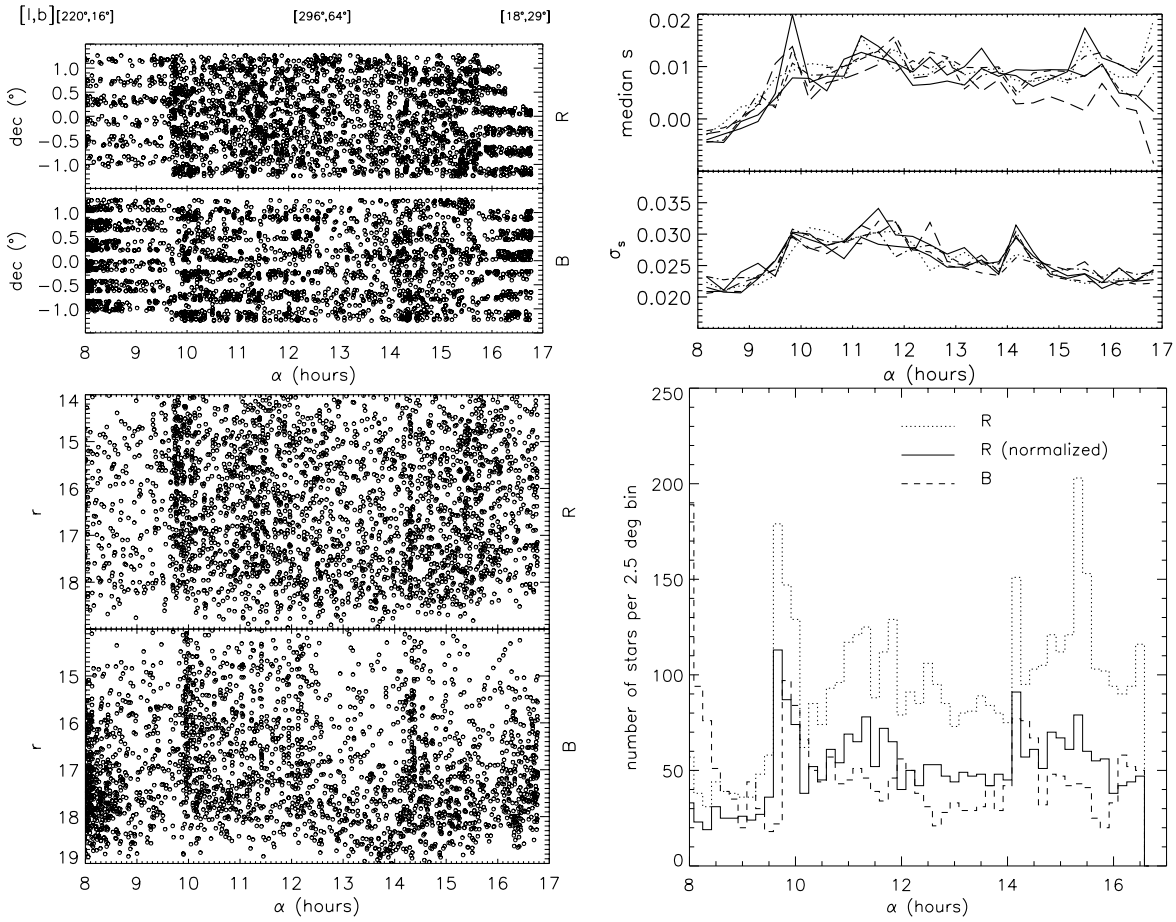

FIG. 2.—*Left panels*: Sky distribution (declination vs. right ascension α) and r magnitude vs. α diagrams for stars in runs 752 and 756 satisfying eq. (4). There are 5125 stars in $\mathscr{R}$ and 2844 in $\mathscr{B}$. Here we have selected a random sample of $\mathscr{R}$ with the same number of stars as in $\mathscr{B}$ for a more direct comparison of the spatial distribution of stars in each subset. The regions $\alpha \lesssim 10^{\rm h}$ and $15^{\rm h}.5 \lesssim \alpha$ contain data from a drift scan that does not have interleaving stripes, hence the very uneven distribution of stars at different declinations in those regions. *Top right panels*: Median value of s and the dispersion as a function of α for the six independent camera columns. We have excluded data closer than 150 pixels to the chip edge because the flat-fielding uncertainties in the u band increase photometric errors by about 1%. *Bottom right panel*: Histograms show the number of stars per 2.°5 bins for the whole $\mathscr{R}$ sample (*dotted curve*), for the $\mathscr{B}$ sample (*dashed curve*), and for a random realization of the $\mathscr{R}$ sample with the same number of stars as $\mathscr{B}$ (*solid curve*).

samples to $\alpha_{\rm J2000.0} = 13^{\rm h}$–$16^{\rm h}$, we find this probability to be $\sim 3 \times 10^{-9}$. If no restriction is applied, the probability is even smaller, $\sim 10^{-10}$. The southern streams of Sagittarius in runs 94 and 125 ($\alpha_{\rm J2000.0} \sim 1^{\rm h}15^{\rm m}$, $\delta_{\rm J2000.0} \sim 0°$; Yanny et al. 2000) and the Draco dwarf spheroidal galaxy in runs 1336/9 and 1356/9 ($\alpha_{\rm J2000.0} = 17^{\rm h}20^{\rm m}$, $\delta_{\rm J2000.0} = 57.°9$; Odenkirchen et al. 2001)—none of which is shown in Figure 2—are recovered as clear overdensities in the distribution of candidate stars, which is not the case for stars in the control sample.

3.2. *Spectroscopic Observations and Analysis*

The results from the previous subsection suggest that the fraction of halo giants in the candidate subset $\mathscr{R}$ is significantly larger than that of the comparison sample $\mathscr{B}$. To investigate this and to derive an estimate of the selection efficiency, we selected stars from two overlapping runs, 125 and 1755, which satisfy the selection criteria in both runs. Of a total of 72 candidates with $\hat{s} > 0.05$, we randomly selected 29, for which we obtained intermediate resolution spectra. The data reduced with the most recent version of photometric pipeline (*photo* version 5_3) have photometric errors of the order 0.02 mag, smaller than the EDR data used here, which have errors of the order 0.03 mag. The requirement that the candidate stars qualify in both runs has a similar effect on efficiency as smaller photometric errors, and thus the selection efficiency obtained here is more representative of the upcoming SDSS Data Release 1.

The r magnitudes of the selected candidates range from 14 to 17 mag, with a median r magnitude of 16 (see Table 1 for the list of stars and their colors). The spectra were obtained during the nights of 2001 October 20–24, using the Calar Alto Faint Object Spectrograph on the Calar Alto 2.2 m telescope in the framework of the Calar Alto Key Project for SDSS Follow-up Observations (Grebel 2001). The resolution was 4 Å, the spectral range $\lambda = 3200$–5800 Å, and we integrated each star for 900 up to 2000 s, depending on the brightness of the star and weather conditions. The reduction process will be described in detail in Paper II.

In the wavelength range probed by the selection method, the features most sensitive to luminosity class are those used by the SPS: the Mg b triplet near 5170 Å and the Ca I λ4227 line. In Figure 3 we show the spectra of six of the stars in the program. With the obtained resolution and signal-to-noise ratios, it is possible to separate the giants from the dwarfs

TABLE 1
SPECTROSCOPICALLY OBSERVED GIANT CANDIDATES

$\alpha_{J2000.0}$	$\delta_{J2000.0}$	$u-g$	$g-r$	r	s	Class
23 22 49.9	00 00 45.6	1.18	0.52	14.57	0.08	G
23 23 30.5	00 58 17.9	1.47	0.75	16.35	0.12	G
23 23 44.0	00 30 16.9	1.32	0.64	14.59	0.12	G
23 25 51.1	01 00 23.0	1.62	0.79	17.06	0.10	D
23 28 57.0	00 55 49.8	1.56	0.50	16.31	0.06	u
23 29 16.7	00 55 51.4	1.31	0.61	16.89	0.08	G
23 31 05.9	00 02 21.7	1.47	0.66	15.27	0.08	D
23 31 22.3	−00 17 32.4	1.33	0.59	16.45	0.07	u
23 34 59.6	−00 16 05.1	1.40	0.62	15.72	0.07	G
23 37 35.1	−01 05 02.5	1.71	0.77	16.68	0.07	D
23 43 56.4	00 10 52.3	1.35	0.58	14.58	0.07	G
23 49 39.7	−00 42 57.0	1.70	0.77	16.42	0.07	D
23 51 53.9	00 02 37.9	1.60	0.71	16.71	0.06	D
00 04 56.7	−00 18 37.0	1.07	0.54	14.67	0.12	G
00 05 7.3	00 02 40.8	1.37	0.62	15.94	0.09	D
00 10 16.9	00 52 25.4	1.71	0.71	14.05	0.06	G
00 15 24.1	−00 21 26.9	1.38	0.69	16.25	0.11	u
00 21 57.5	−00 17 38.5	1.23	0.52	14.75	0.07	G
00 29 00.8	00 05 29.5	1.42	0.59	14.77	0.06	G
00 30 05.8	−00 24 07.2	1.62	0.78	16.53	0.10	D
00 32 20.1	00 51 41.4	1.09	0.48	16.17	0.07	G
00 32 31.5	−00 22 27.2	1.61	0.72	16.47	0.06	D
00 33 36.4	−00 49 08.7	1.42	0.57	14.38	0.06	D
00 33 40.5	−00 17 17.5	1.42	0.62	14.13	0.08	D
00 34 28.4	00 32 04.3	1.47	0.69	16.03	0.09	D
00 35 44.5	00 04 12.4	1.30	0.54	15.19	0.06	G
00 38 21.8	−00 17 48.4	1.35	0.56	14.02	0.07	D
00 38 39.2	00 07 12.9	1.64	0.69	14.91	0.06	D
00 38 42.4	00 35 55.1	1.23	0.55	16.11	0.07	u

NOTES.—Right ascension, declination, apparent magnitudes, and colors of the 29 candidates with follow-up spectra. Units of right ascension are hours, minutes, and seconds, and units of declination are degrees, arcminutes, and arcseconds. The last column denotes whether the star is a giant (G) or dwarf (D) or whether the spectra was not good enough to determine the luminosity class (u).

even by simple visual inspection. The three spectra in the left panels clearly show the absence of the MgH and Mg *b* triplet (compare to the spectra shown in the right panel), thus proving that at least some of the stars in our sample are giants. To obtain a more quantitative discrimination between giant and dwarf stars, we also measure the equivalent widths of the Ca II K, the Ca I λ4227 and the Mg *b* triplet lines, according to the definitions of Morrison et al. (2002). We use their calibrations to assign luminosity class. Out of the 29 observed stars, 12 are metal-poor giants, 13 are metal-poor dwarfs, and for four stars the obtained signal-to-noise ratio is insufficient for classification. A rough estimate of [Fe/H] has been obtained by visual inspection of the spectra (we do not have enough standards for proper calibration). Such a method has an inherent uncertainty of about 0.5 dex.

We conclude that the identification of metal-poor giants can be made with satisfactory efficiency, of order 50%, using the SDSS photometric data. However, we caution that the stars in our spectroscopic sample are relatively bright ($r < 17$), and thus this efficiency will be lower than 50% for fainter magnitudes due to increased photometric errors and contamination by subdwarfs.

4. DISCUSSION

The technique described in this paper can be used to study the structure of the Galactic halo in two complementary ways. One method is to select candidates for spectroscopic follow-up and determine their luminosity class and radial velocity. The latter essentially adds an extra dimension that could prove useful in disentangling structures in the halo (Harding et al. 2001). This approach would be analogous to that used by the SPS. A second possibility, and which perhaps makes a better use of the uniquely large SDSS data set, is a statistical approach. One can compare the angular and

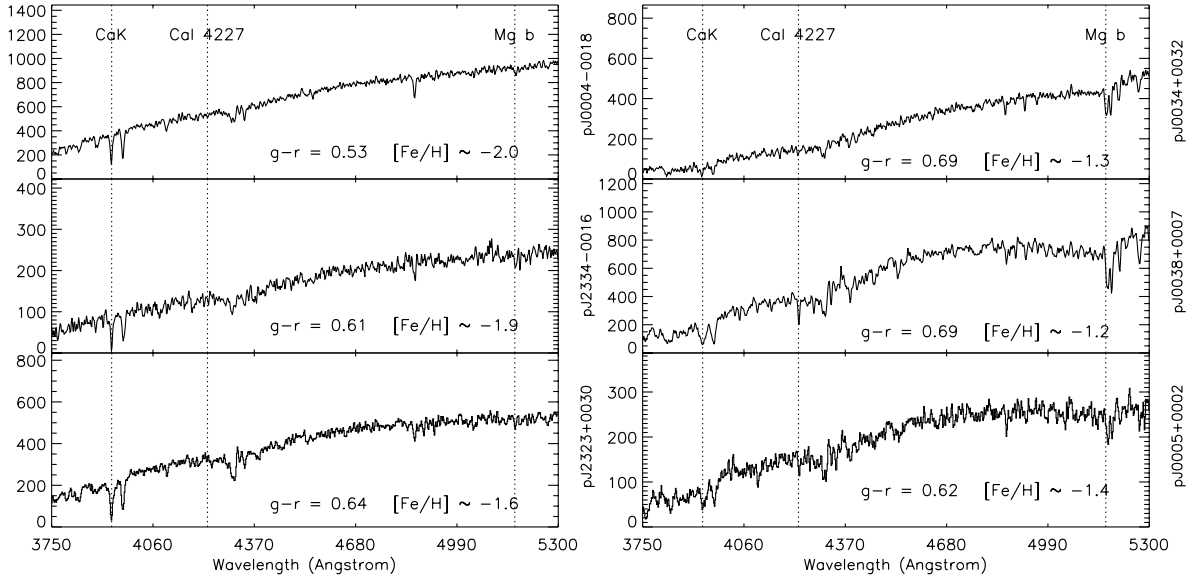

FIG. 3.—Spectra of six candidate stars, which were observed with the 2.2 m telescope at Calar Alto. The spectra have 4 Å resolution and have not been flux calibrated. *Left panels*: Spectra of three giants. *Right panels*: Spectra of three dwarfs. Notice the strong MgH and Mg *b* triplet in the dwarfs, which are almost absent in the giants. The candidate stars have characteristic colors with median $g-r = 0.62$, which typically corresponds to a $T_{\rm eff} \sim 5000$ K, median $u-g = 1.40$, and median $s = 0.07$. Their median r magnitude is 16.03.

magnitude distributions of candidate giant stars with that of stars in a control sample, in the same spirit as Figure 2. A statistical subtraction of the distributions of the data sets may allow, for example, a mapping of overdensities in the number of candidate giant stars at different locations in the sky. When combined with other techniques for selecting halo stars, such as RR Lyrae stars and blue horizontal-branch stars, it will be possible to produce an unprecedented, detailed three-dimensional map of the Galactic halo based on the SDSS imaging survey.

We are especially grateful to Heather Morrison and the rest of the SPS collaboration for providing us with a list of giants from the Spaghetti survey and for very useful discussions. Ž. I. and R. H. L. acknowledge generous financial support and constant encouragement by G. R. K., and Ž. I. thanks the Max Planck Institute for Astrophysics (MPA) for hospitality. We also thank Stefano Zibetti for help in setting up IRAF at MPA. D. P. S. was supported in part by National Science Foundation grant AST 99-00703. The spectroscopic observations were made in the framework of the Calar Alto Key Project for SDSS Follow-up Observations at the German-Spanish Astronomical Centre, Calar Alto Observatory, operated by the Max Planck Institute for Astronomy, Heidelberg, jointly with the Spanish National Commission for Astronomy. Funding for the creation and distribution of the SDSS Archive has been provided by the Alfred P. Sloan Foundation, the Participating Institutions, the National Aeronautics and Space Administration, the National Science Foundation, the U.S. Department of Energy, the Japanese Monbukagakusho, and the Max Planck Society. The SDSS is managed by the Astrophysical Research Consortium (ARC) for the Participating Institutions: the University of Chicago, Fermilab, the Institute for Advanced Study, the Japan Participation Group, the Johns Hopkins University, Los Alamos National Laboratory, the Max Planck Institute for Astronomy, the Max Planck Institute for Astrophysics, New Mexico State University, Princeton University, the United States Naval Observatory, and the University of Washington.

REFERENCES

Beers, T. C., Rossi, S., Norris, J. E., Ryan, S. G., & Shefler, T. 1999, AJ, 117, 981
Dohm-Palmer, R. C., et al. 2001, ApJ, 555, L37
Fan, X. 1999, AJ, 117, 2528
Finlator, K., et al. 2000, AJ, 120, 2615
Flynn, C., & Morrison, H. L. 1990, AJ, 100, 1181
Fukugita, M., Ichikawa, T., Gunn, J. E., Doi, M., Shimasaku, K., & Schneider, D. P. 1996, AJ, 111, 1748
Geisler, D. 1984, PASP, 96, 723
Geisler, D., Claria, J. J., & Minniti, D. 1991, AJ, 102, 1836
Grebel, E. K. 2001, Rev. Mod. Astron., 14, 223
Gunn, J. E., et al. 1998, AJ, 116, 3040
Harding, P., Morrison, H. L., Olszewski, E. W., Arabadjis, J., Mateo, M., Dohm-Palmer, R. C., Freeman, K. C., & Norris, J. E. 2001, AJ, 122, 1397
Helmi, A., White, S. D. M., & Springel, V. 2003, MNRAS, in press (astro-ph/0208041)
Hogg, D. W., Finkbeiner, D. P., Schlegel, D., & Gunn, J. E. 2002, AJ, 122, 2129
Ivezić, Ž., et al. 2000, AJ, 120, 963
Johnston, K. V., Hernquist, L., & Bolte, M. 1996, ApJ, 465, 278
Kinman, T. D., Suntzeff, N. B., & Kraft, R. P. 1994, AJ, 108, 1722
Lenz, D. D., Newberg, H. J., Rosner, R., Richards, G. T., & Stoughton, C. 1998, ApJS, 119, 121
Lupton, R. H., et al. 2001, in ASP Conf. Proc. 238, Astronomical Data Analysis Software and Systems X, ed. F. R. Harnden, Jr., F. A. Primini, & H. E. Payne (San Francisco: ASP), 269
Majewski, S. R., Ostheimer, J. C., Kunkel, W. E., & Patterson, R. J. 2000, AJ, 120, 2550
Martinez-Delgado, D., Aparicio, A., Gómez-Flechoso, M. A., & Carrera, R. 2001, ApJ, 549, L199
Mayer, L., Moore, B., Quinn, T., Governato, F., & Stadel, J. 2002, MNRAS, 336, 119
Mihalas, D., & Binney J. 1981, Galactic Astronomy: Structure and Kinematics (San Francisco: Freeman), 120
Morrison, H. L., et al. 2000, AJ, 119, 2254
———. 2002, AJ, submitted
Newberg, H. J., et al. 2002, ApJ, 569, 245
Odenkirchen, M., et al. 2001, AJ, 122, 2538
Paltoglou, G., & Bell, R. A. 1994, MNRAS, 268, 793
Pier, J. R., et al. 2003, AJ, in press
Robin, A. C., Reylé, C., & Crézé, M. 2000, A&A, 359, 103
Schlegel, D. J., Finkbeiner, D. P., & Davis, M. 1998, ApJ, 500, 525
Smith, J. A., et al. 2002, AJ, 123, 2121
Sommer-Larsen, J., Flynn, C., & Christensen, P. R. 1994, MNRAS, 271, 94
Steinmetz, M., & Navarro, J. F. 2002, NewA, 7, 155
Stoughton, C., et al. 2002, AJ, 123, 485 (EDR)
Vivas, A. K., et al. 2001, ApJ, 554, L33
Willman, B., Dalcanton, J., Ivezić, Ž., Jackson, T., Lupton, R., Brinkmann, J., Henessy, G., & Hindsley, R. 2002, AJ, 123, 848
Yanny, B., et al. 2000, ApJ, 540, 825
York, D. G., et al. 2000, AJ, 120, 1579